Spin polarized transport in nanoscale devices

András Halbritter, Attila Geresdi and György Mihály*

Received Xth XXXXXXXXXX 20XX, Accepted Xth XXXXXXXXX 20XX
First published on the web Xth XXXXXXXXXX 200X
DOI: 10.1039/b000000x

Recently, tremendous fundamental and technological interest has been created by the possible use of the spin degree of freedom of electrons for information processing. This field, often referred to as spintronics, is rapidly developing: new ideas and promising materials emerge, which - taking advantage of the broadening facilities of nanotechnology - offer novel sensor, memory and even logics applications. In this article we review some intriguing aspects of spin-related transport at nanoscale. First the basic concept of spin polarized transport and the calculation of the current spin polarization is demonstrated within the framework of the Landauer formalism. Next the experimental method of point contact Andreev spectroscopy is reviewed, which is capable of resolving both the current spin polarization and the spin diffusion length. Finally the most widely utilized application of spin polarized transport, the spin valve structure is discussed.

1 Introduction

The spin dependence of electronic transport is hidden in most metals. However, spin polarized current injected to a nonmagnetic conductor keeps the spin memory within a certain distance, typically in the submicron range. By now, nanoscale devices have been prepared where the size of the components is well below the distance of the spin-memory, and both the control of the spin states and the utilization of the spin information have been demonstrated.[1,2] In most of these electronic applications ferromagnetic components act as spin filter and detector,[3,4] while a nonmagnetic metal mediates the spin information: this is the simplest spin-valve structure. For the design of such nanodevices a proper understanding of spin dependent transport is necessary, including the knowledge of the carriers' spin-polarization, or the determination of the spin diffusion length.

In the first part of this review we present a simple model for the spin dependent transmission through a nanostructure based on the Landauer formalism widely applied in the field of nanophysics. In the second part a special measurement technique is reviewed, which allows the direct determination of the current spin polarization, and with which even the decay of the spin polarization i.e. the spin diffusion length can be determined in a nonmagnetic layer. In the last part the nanoscale spin-valve architecture is discussed, demonstrating how the results of basic research find broad technical application and trigger an intensive development of novel memory elements.

Department of Physics, Budapest University of Technology and Economics and Condensed Matter Research Group of the Hungarian Academy of Sciences, 1111 Budapest, Budafoki út 8, Hungary. E-mail: mihaly@phy.bme.hu

2 Spin dependent transport in nanostructures

In a macroscopic conductor the electrons suffer numerous scattering processes as they move from one electrode towards the other. Due to the scattering on impurities and lattice defects the drift momentum of the electrons gained from the electric field is lost. This process is described by the characteristic length scale of the momentum relaxation mean free path, l_m. Inelastic scattering processes like the scattering on lattice vibrations lead to a change of energy, which results in the loss of phase coherence for electron waves. The corresponding characteristic length scale is called phase diffusion length, l_ϕ.[5,6] Within a large enough distance the electrons also loose their spin information, as characterized by the spin diffusion length, l_s.[3,7] In a nanostructure, however, all these length scales may become comparable to, or even larger than the characteristic size of the structure, L. For instance, in small enough structures ($L < l_s$) the spin information is preserved, which is a key ingredient for spintronic applications.[8] For structures smaller than l_ϕ coherent quantummechanical features appear, whereas for $L < l_m$ a ballistic transport is observed, i.e. the electrons scatter only on the edges of the structure, but not inside.

Here we give a simple model to demonstrate how spin-polarized current may arise in ferromagnetic nanostructures, which are smaller than the spin diffusion length. In order to provide a microscopic insight to the relevant processes we use the well established approach of the Landauer formalism,[6,9] which has been successfully applied to describe several nanoscale systems, like atomic-sized conductors[10] or semiconductor nanostructures.[11,12]

As a simplified model first we consider an ideal two dimensional wire with parallel walls (Fig. 1(a)). In the ballistic limit

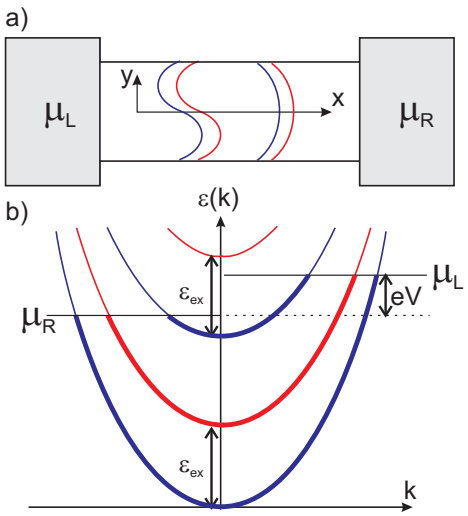

Fig. 1 *Panel (a) demonstrates an ideal 2D quantum wire with parallel walls and the absence of scattering inside the wire. The standing waves demonstrate the quantized transverse modes in the wire. Panel (b) demonstrates the dispersion of the conductance channels inside the wire in a free electron picture. The blue parabolas correspond to spin up electrons, whereas the red parabolas stand for the spin down electrons. The two spin subbands are shifted by an energy ε_{ex}. The thick/thin lines denote the occupied/unoccupied states. Note, that right going states ($k > 0$) are occupied up to an energy higher by eV than the left moving states ($k < 0$).*

no scattering occurs in the wire, and an electron entering into the wire from one side will propagate to the other side without changing its energy and spin state. Along the wire (x-direction) the electrons exhibit a free, reflectionless propagation, whereas perpendicular to the wire (y-direction) quantized transverse modes are formed. In this simple geometry the wavefunction factorizes to the product of a longitudinal and a transverse wave function, and the energies corresponding to the transverse standing waves and the longitudinal propagation are simply added. After including magnetism in a Stoner type picture the energy dispersion for this system can be written as:

$$\varepsilon_n^\sigma(k) = \varepsilon(k) + \varepsilon_n - \sigma\varepsilon_{\rm ex}, \qquad (1)$$

where ε_n is the energy corresponding to the quantized transverse modes, $\varepsilon(k)$ is the dispersion of the extended Bloch states in the x direction (k=k_x), $\sigma = \pm 1/2$ is the spin index, and $\varepsilon_{\rm ex}$ is the exchange energy. The resulting dispersion is a set of one dimensional dispersion curves, which are vertically shifted by the transverse energies and the exchange energy (Fig. 1(b)). The discrete one dimensional dispersions are called *conductance channels*.[6,13]

In such an ideal wire the states with positive and negative k are well separated, the former are all coming from the left electrode, while the latter are all coming from the right electrode. In a symmetric situation no net current flows. Application of a bias voltage between the two sides of the wire, however, shifts the chemical potentials of the right and left moving electron states by eV with respect to each other, and this imbalance results in a finite current. For a selected conductance channel the velocity of the electrons and the density of states is respectively given as

$$v_n^\sigma = \frac{1}{\hbar}\frac{\partial\varepsilon_n^\sigma(k)}{\partial k}, \quad g_n^\sigma = \frac{L}{2\pi}\left(\frac{\partial\varepsilon_n^\sigma(k)}{\partial k}\right)^{-1}, \qquad (2)$$

where L is the length of the nanowire. The spacial density for the electron states in the eV energy window is obtained as

$$n_n^\sigma = eVg_n^\sigma/L. \qquad (3)$$

The current is then calculated as a product of charge, velocity and electron density, summing over the spins and all the conductance channels:

$$I = \sum_\sigma \sum_{n=1}^{M^\sigma} ev_n^\sigma n_n^\sigma = \sum_\sigma \frac{e^2}{h} M^\sigma V. \qquad (4)$$

Here M^σ is the number of open conductance channels, i.e. the number of 1D dispersion curves crossing the Fermi energy for a given spin orientation. Note that $\partial\varepsilon/\partial k$ cancels in the product of v and n, thus the above result is valid for any shape of the dispersion curve. Furthermore, the two dimensional model only simplifies the visualization, but the above arguments also hold for any perfect three dimensional nanowire with uniform cross section along the x axis.

Here we have taken advantage of the assumption that the spin state is conserved, i.e. the structure is smaller than the spin diffusion length. This has allowed the separation of the current to a purely spin up and a purely spin down component being two independent *routes* of the transport: $I = I^\uparrow + I^\downarrow = (e^2/h)(M^\uparrow + M^\downarrow)V$. The total current is determined by the number of open conductance channels, and the conductance ($G = I/V$) is an integer multiple of $e^2/h = (25.8\,\mathrm{k\Omega})^{-1}$.

Due to the shifted spin subbands, $M^\uparrow$ not necessarily equals $M^\downarrow$. This is indicated by Fig. 2, where only the linearized part of the 1D dispersions around the Fermi energy is shown demonstrating that the free electron dispersions in Fig. 1(b) are only illustrations and are generally not considered in this model. The degree of the resulting spin polarization can be characterized by the ratio of the spin polarized current and the total current:

$$P_c = \frac{I^\uparrow - I^\downarrow}{I^\uparrow + I^\downarrow} = \frac{M^\uparrow - M^\downarrow}{M^\uparrow + M^\downarrow}. \qquad (5)$$

This normalized current spin polarization can reach even 100% ($P_c = 1$) in case of a half-metal, where only one type of carrier is present at the Fermi level.

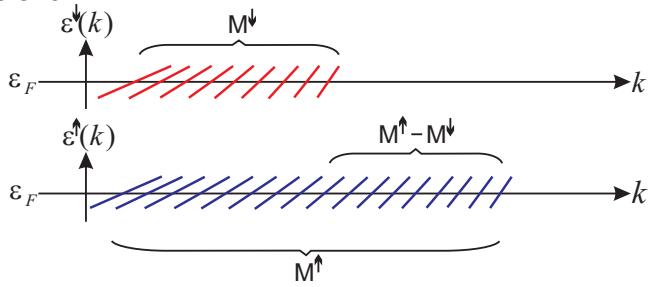

Fig. 2 *The dispersion curves around the Fermi energy for the different conductance channels. The bottom and top panels correspond to spin up and spin down electrons, respectively. Due to the exchange splitting the number of open conductance channels differs for the two spin subbands.*

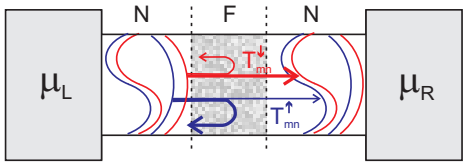

Fig. 3 *A diffusive ferromagnetic region is sandwiched between two normal metal ideal quantum wires. The transport is determined by spin dependent transmission probabilities between the conductance channels at the two sides.*

A more realistic description can be given for the conductance of a piece of magnetic nanowire inserted between non-magnetic reservoirs by taking also into account elastic scatterings (Fig. 3). According to the Landauer picture the transport in this system can be be described by the transmission probabilities T_{nm}, i.e. the probability for the transmission of an electron from channel n on the left side to channel m on the right side. These transmission probabilities depend on the "waveguide" parameters of the wire. While $T_{nm} = \delta_{nm}$ corresponds to the previous model of an ideal wire, $T < 1$ represents scatterings in the wire due to defects, impurities, etc.

As no spin mixing occurs between the spin up and spin down states, the current can still be calculated for each spin state independently taking into account the finite transmissions of the channels:[6,10,13]

$$I^\sigma = \frac{e^2}{h} \sum_{n,m=1}^{M^\sigma} T^\sigma_{nm} V. \tag{6}$$

The values of T_{nm} depend on the Fermi wave numbers of the involved channels. Due to the spin-dependent shift of the dispersions the spin up and the spin down channels have different wave numbers at the Fermi energy. Thus, in general, the transmission probability may become spin dependent even without any direct spin-interaction, like spin-orbit coupling.

The spin dependent current can be rewritten in the form:

$$I^\sigma = \frac{e^2}{h} M^\sigma \bar{T}^\sigma V, \tag{7}$$

where $\bar{T}^\sigma$ is the average transmission probability for all the conductance channels with a given spin direction. With this notation the spin polarization of the current can be written as:

$$P_c = \frac{I^\uparrow - I^\downarrow}{I^\uparrow + I^\downarrow} = \frac{M^\uparrow \bar{T}^\uparrow - M^\downarrow \bar{T}^\downarrow}{M^\uparrow T^\uparrow + M^\downarrow T^\downarrow}. \tag{8}$$

It is evident from this formula, that either the difference of the transmission probabilities for the two spin channels, or the difference in the number of open channels for spin up and spin down electrons gives contribution to the spin polarization of the current.

In case of a few conductance channels the difference in $\bar{T}^\uparrow$ and $\bar{T}^\downarrow$ may introduce a spin polarized current even for the same number of open channels. Indeed, for ferromagnetic atomic point contacts, the transmission probabilities for the two spin channels are expected to differ significantly.[14]

However, for larger structures, where many conductance channels are present (Fig. 2), $\bar{T}^\sigma$ is an average over a broad ensemble of different wavenumbers, and for diffusive junctions random matrix theory (RMT) predicts a universal value of $\bar{T}^\sigma = l^\sigma_m / L$,[15] where L is the length of the diffusive region. As the momentum relaxation mean free path is expected to be similar for the two spin subbands, $\bar{T}^\uparrow \approx \bar{T}^\downarrow$ can be assumed. Accordingly the key contribution to the spin polarization is given solely by the difference of $M^\uparrow$ and $M^\downarrow$. In this limit, Eq. 5 gives a reasonable approximation for the spin polarization, even for non-ideal transmission probabilities ($\bar{T}^\uparrow \approx \bar{T}^\downarrow < 1$).

According to Eq. 2 the number of conductance channels can be formally written as:

$$M^\sigma = \frac{2\pi\hbar}{L} \sum_{n=1}^{M^\sigma} v^\sigma_n g^\sigma_n. \tag{9}$$

Introducing a mean Fermi velocity, which is the average of the Fermi velocities for the different conductance channels weighted by the density of states of the channels,

$$\bar{v}^\sigma_F = \frac{\sum_n g^\sigma_n v^\sigma_n}{\sum_n g^\sigma_n}, \tag{10}$$

and noting that $\sum_n g^\sigma_n = g^\sigma_F$ is the total density of states at the Fermi level, the formula for the current spin polarization can be rewritten as:

$$P_c \approx \frac{M^\uparrow - M^\downarrow}{M^\uparrow + M^\downarrow} = \frac{g^\uparrow_F \bar{v}^\uparrow_F - g^\downarrow_F \bar{v}^\downarrow_F}{g^\uparrow_F \bar{v}^\uparrow_F + g^\downarrow_F \bar{v}^\downarrow_F}. \tag{11}$$

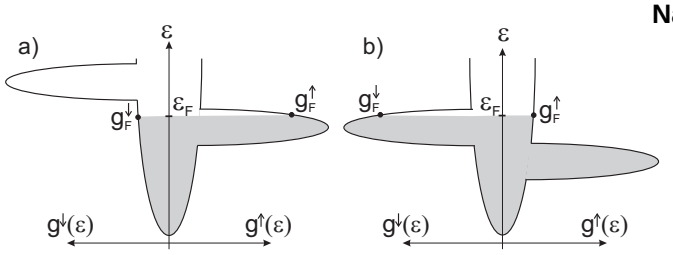

Fig. 4 *Illustration for the density of states in ferromagnets. The magnetism is related to the exchange splitting of the narrow d (or f) bands. Panel (a) demonstrates the DOS in Fe: for minority spins (left side) the d band is above the Fermi level, whereas for majority spins (right side) the Fermi level lies inside the d band. Accordingly the DOS is significantly larger for the majority spins. Panel (b) demonstrates the DOS for Co and Ni type band filling. In this case ε_F is above the d band for majority spins, whereas it lies inside the d band for minority spins resulting in a negative Fermi surface spin polarization with respect to the positive magnetization.*

This formula supplies a microscopic background for the conventional formulation of the current spin polarization[16] expressed by Fermi surface parameters of the two spin subbands: density of states and Fermi velocity.

In real ferromagnets the exchange splitting of narrow *d* (or *f*) bands and the filling of the bands determine the magnetic properties (see Fig. 4). The integral of the density of states up to the Fermi energy is different for the two spin orientations, which results in a finite magnetization, conventionally selecting the up spin as the majority spin orientation. However, the electron transport is determined by the Fermi surface properties. The spin polarized transport is not characterized by the magnetization, rather it is described by the spin polarization of the current as described by Eq. 11. An interesting example is supplied by the Co or Ni type band fillings: the density of states at the Fermi level is much larger for the down spin, leading to a situation where the current spin polarization may take a sign opposite to that of the magnetization (Fig. 4b).

3 Measurement of the current spin polarization and the spin diffusion length

As shown in the previous section, there is an important difference between magnetization and current spin polarization. This difference highlights that magnetization measurements – for which various sensitive tools are available – are not an appropriate tool for the study of spin-polarized transport. Somewhat closer information can be obtained by spin resolved photoemission spectroscopy, which measures the density of states spin polarization, $P_{DOS} = (g_F^{\uparrow} - g_F^{\downarrow})/(g_F^{\uparrow} + g_F^{\downarrow})$.[17] Nevertheless, for a close insight to the current spin polarization, direct transport measurements are necessary. There are several transport measurements reveling various consequences of spin polarized currents,[18–22] but for a direct measurement of P_c a few methods are available. In the following we demonstrate such a method based on point contact Andreev spectroscopy. (An alternative method is based on superconducting tunneling spectroscopy in external magnetic field.[23])

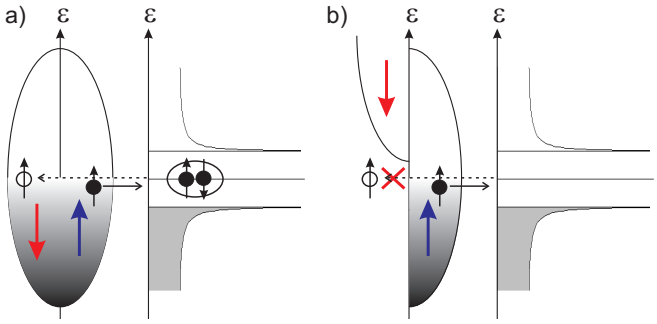

Fig. 5 *Panel (a): Illustration of Andreev reflection between a nonmagnetic metal and a superconductor. The incoming spin up electron is reflected as a spin down hole, and meanwhile a Cooper pair is created in the superconductor. Panel (b) demonstrates the absence of Andreev reflection between a fully spin polarized ferromagnet (half metal) and a superconductor. In this case no spin down states are available, and the Andreev reflection of the incoming spin up electrons is completely suppressed.*

The basic idea of Andreev spectroscopy is to measure the Andreev reflection of spin polarized conduction electrons on a superconductor surface.[24–26] When current is injected into the superconductor the charge must be converted to spin singlet Cooper pairs composed from two electrons with opposite spins. On the normal side an incoming electron drags an other electron with opposite spin and momentum, which is equivalent to reflecting a hole with opposite spin and momentum. This process is called Andreev reflection (Fig. 5(a)). Compared to the single particle transfer (which occurs at voltages above the superconductor gap energy, $|eV| > \Delta$), in the Andreev reflection double charge quanta are transmitted, and therefore the zero bias conductance may be even twice the high-bias, normal-state conductance. However, for a spin polarized metal the spin states available for the reflected hole are reduced (see Fig. 5(b)), and the conductance is suppressed.

The above idea was successfully used to get a direct experimental measure of the current spin polarization in various ferromagnetic metals[16,24–32] as well as more complex material systems, such as dilute magnetic semiconductors.[33,34] In a real structure, however, a non-perfect barrier should also be considered between the ferromagnet and the superconductor. Different models have been set up to describe the shape of the current voltage characteristics of ferromagnet - superconductor nanojunctions as a function of the current spin polarization (P_c) and the transparency of the interface (T). In the

most widely applied method the original Blonder-Tinkham-Klapwijk (BTK) theory of the Andreev reflection[35] is extended for ferromagnetic materials splitting the current to unpolarized and fully polarized parts, and then assuming no Andreev reflection for the fully polarized part and applying the BTK theory for the unpolarized part.[28] In an other approach spin-dependent transmission coefficients are considered, and their imbalance is deduced from the analysis of the $I-V$ characteristics.[26,36]

Experimentally the ferromagnet - superconductor interface is either created in an STM geometry by pushing a superconducting tip to a magnetic sample,[24,28,29] or a nano-hole is fabricated in an isolating membrane, and afterwards the ferromagnetic and the superconducting layers are evaporated to the two sides of this hole.[25,26,30]

To demonstrate the experimental determination of the current spin polarization Fig. 6 shows the results of our study on a Fe-Nb nanojunction created in the tip - sample geometry. In panel (a) the experimental differential conductance curve is fitted by the modified BTK theory revealing a current spin polarization of $P_c = 0.62$. This value is somewhat higher than the result of earlier studies,[24,28] which may arise form the different surface preparation: in contrast to previous studies in our measurements a protective Au surface layer with a thickness of 5 nm was applied to prevent the contamination of the Fe surface. The figure also demonstrates the precision of the method: if the spin polarization is fixed at a value slightly detuned from the optimal fit, no satisfactory fit is available by varying the barrier transparency (T). It is also found that the two theoretical models lead to essentially identical spin polarization values, even though they mathematically cannot be mapped onto each other.

Another experimental example is presented in Fig. 7(a), demonstrating a differential conductance curve on Co-Nb junction. For cobalt the spin polarization is smaller than for iron: based on numerous measurements on various junctions $P_c = 0.41 \pm 0.04$ is obtained. This value agrees well with previous measurements performed on nano-hole samples.[26]

It is worth noting, that the fitting functions contain two additional parameters: the temperature and the superconducting gap. We have found that for junctions in the ballistic limit the fitting results in a temperature which agrees well with the experimental temperature value. The gap also coincides with the bulk Nb gap, and the BCS temperature dependence of the gap[37] is clearly resolved by fitting the differential conductance curves at various temperatures (see Fig. 7(b)). This consistency of the method is, however, lost if the contact size is increased and junctions in the diffusive limit are studied.[34] In this regime a considerable smearing of the curves is observed, and good fits are only possible if the fitting temperature is significantly larger than the experimental value. In extreme cases the fitting temperature may even grow above the critical temperature of Nb, which is an obvious contradiction.

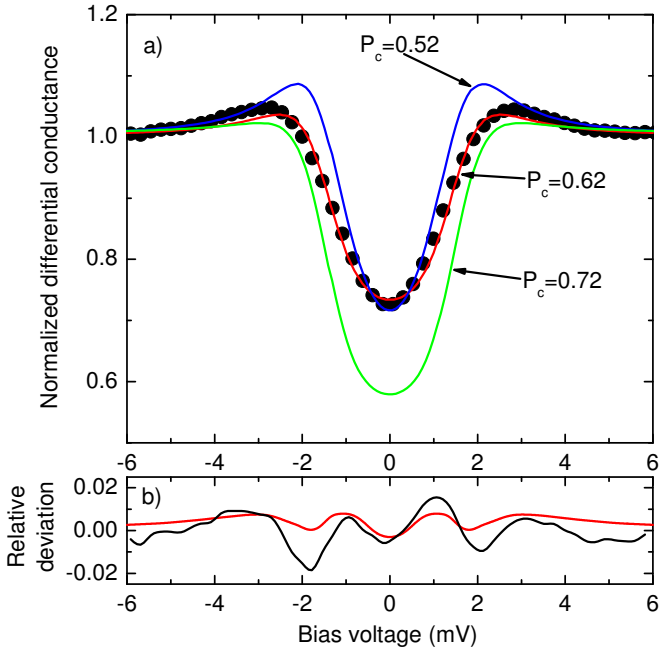

Fig. 6 *Panel (a) demonstrates the differential conductance curve measured between an Fe sample covered with 5 nm Au capping layer and a Nb tip. The red line shows the best fit using the modified BTK theory, yielding a normal state resistance of $R_N = 890\,\Omega$, a spin polarization of $P_c = 0.62$, a contact transparency of $T = 0.98$, a superconducting gap of $\Delta = 1.50\,meV$ at a temperature of $T = 4.2\,K$. Note, that the normalized barrier strength, Z in the BTK theory is converted to transmission probability as $T = (1+Z^2)^{-1}$. The blue and green lines show fits, where P_c is fixed at values intentionally detuned from the best fitting value, and only T is used as a fitting parameter. These curves demonstrate that the resolution of the method is well below $\Delta P_c = 0.1$. Panel (b) demonstrates the deviation between the best fits based on the modified BTK theory and the Hamiltonian approach (red line). Although these two models do not give exactly the same fit, their deviation is smaller than the deviation of the experimental curve from the modified BTK fit (black line).*

The above examples provide an insight to spin polarization measurement based on Andreev spectroscopy. This method provides a sensitive and reliable method for the direct determination of P_c if small ballistic junctions are used. For such junctions it is generally found that the results are not sensitive to the choice of the fitting model. However, for larger diffusive junctions the quality of the fits is significantly worse and accordingly the reliability of the method breaks down. Another requirement for the reliability of the method is the choice of a transparent junction. As Andreev reflection is a second order process, for low transparency junctions ($T \ll 1$) its probability is suppressed and the differential conductance curve is not

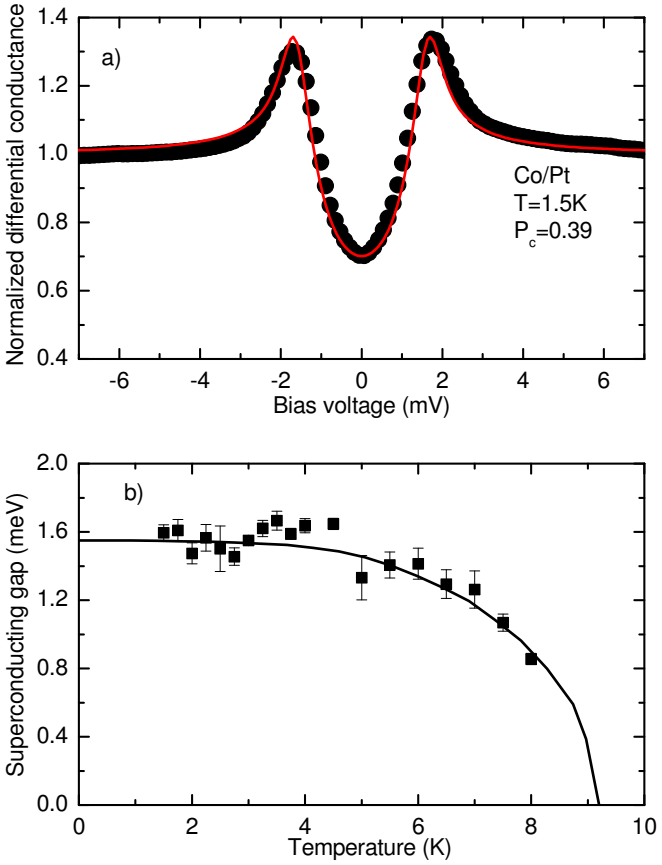

Fig. 7 *Panel (a) demonstrates the differential conductance curve for a nanojunction between a Nb tip and a Co sample with a Pt capping layer. The best fit (red line) yields* $R_N = 780\,\Omega$ $P_c = 0.39$, $T = 0.87$, $\Delta = 1.62\,meV$ *at a temperature of* $1.5\,K$. *Panel (b) demonstrates the temperature dependence of the fitted gap values clearly following the BCS prediction.*

sensitive to the degree of spin polarization.

It is worth emphasizing that Andreev spectroscopy acts as a local probe technique, it is able to probe the spin polarization locally, at the nanometer scale.[34] In this sense it can be also applied to detect the lateral variations of the spin polarization.

Next we show how the spin diffusion length can be determined by Andreev spectroscopy.[38] For this purpose a nonmagnetic capping layer is evaporated on the top of the ferromagnetic sample. The degree of spin polarization is measured at the surface of the capping layer, studying the decay of the spin polarization as the thickness of the capping layer is systematically increased. The carrier spin polarization is expected to decay exponentially as a function of the layer thickness. Fig. 8 shows the results for Fe/Au samples clearly resolving this exponential decay, and yielding a spin diffusion length of $53 \pm 6\,nm$. This example further demonstrates that Andreev spectroscopy is a powerful tool to measure current spin polarization, and it may find even wider application as a local probe technique to study the lateral variation of P_c at nanometer scale.

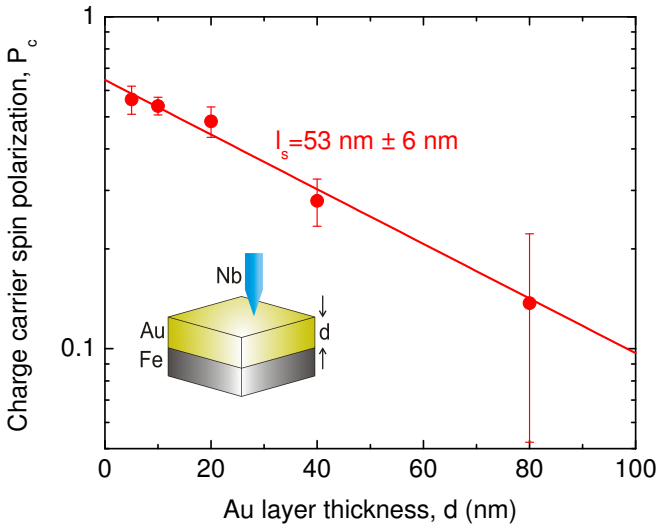

Fig. 8 *The measurement of spin diffusion length by Andreev spectroscopy. The inset demonstrates the experimental setup: on the top of Fe samples Au capping layers are evaporated with varying thickness. The current spin polarization is measured at the top of the Au layer as a function of the layer thickness. Each point in the figure corresponds to more than 10 independent junctions, which were created by lateral shifting the sample below the lifted Nb-tip by a piezo actuator. The error bars represent the scattering of the calculated polarization values for these independent experiments. The exponential decay of the spin polarization is clearly resolved as the Au layer thickness is increased yielding a spin diffusion length of* $53 \pm 6\,nm$.

4 The spin valve structure

The knowledge of current spin polarization and spin diffusion length is essential for the design of spintronic devices. In the previous part we have shown an experimental method which allows the determination of both quantities. In the following we turn to the application of spin polarized transport by discussing the most widely utilized spintronic device, the nanoscale spin-valve structure. First we give simple demonstrative models for this structure, and then we briefly discuss possible applications for next generation data storage devices.

The basic idea of this structure dates back to the discovery of the giant magnetoresistance (GMR) effect by Albert Fert[39] and Peter Grünberg[40], for which the Nobel price in physics was awarded in 2007. The architecture is based on two ferromagnetic layers, which are separated by a paramagnetic layer being thinner than the spin diffusion length (Fig. 9(a)). It was

found that the conductance of this device is larger for the parallel orientation of the two magnetic layers than for the antiparallel orientation.

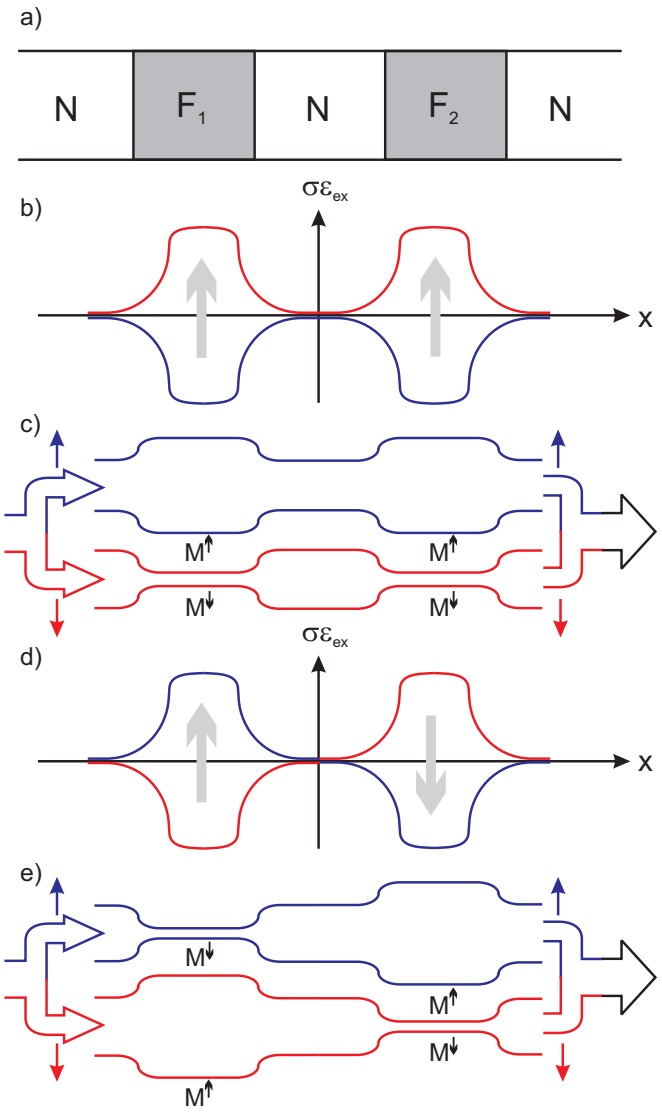

Fig. 9 *Panel (a) demonstrates the basic idea of a spin valve structure: two ferromagnetic regions are separated by a narrow normal region, and this structure is connected to normal leads at both sides. Panels (b,d) demonstrate the variation of the exchange energy along the structure. Panel (b) corresponds to the parallel magnetic orientation of the layers (both layers have ↑ magnetic orientation), whereas panel (d) demonstrates the antiparallel orientation (↑ in the first layer and ↓ in the second one). Panels (c) and (e) respectively show the equivalent ballistic model, where the change of the exchange energy is replaced by an effective narrowing or widening of the channel.*

To understand this phenomenon, as the simplest model we can consider an ideal quantum wire, in which the exchange coupling is switched on adiabatically in two regions (Fig. 9(b,d)). The parallel orientation is modeled by a positive exchange in both regions, whereas the antiparallel orientation corresponds to opposite signs of the exchange in the two regions. Similarly to the previous situations the current can be divided to two independent components corresponding to spin up and spin down electrons. For a given spin orientation the effect of the exchange energy is very similar to an effective spatial narrowing or widening of the channel, which would increase/decrease the transverse quantized energies (Fig. 9(c,e)). Therefore the system can be considered as serial connected quantum point contacts. For electrons with majority spin direction (spin direction parallel to the magnetization direction) the number of open channels is denoted by $M^{\uparrow}$, whereas for minority spins (antiparallel spin direction to the magnetization direction) the number of open channels is $M^{\downarrow}(< M^{\uparrow})$. (Note, that here the superscript $\uparrow$ denotes majority orientation instead of the real spin direction, and the number of open channels is also $M^{\uparrow}$ for down spins in down oriented magnetization of the magnetic layer.)

In such ballistic quantum point contacts the conductance is determined by the number of modes at the narrowest cross section. If the two magnetic layers have antiparallel (AP) orientation either the first or the second layer restricts the number of channels to $M^{\downarrow}$, and so the conductance for both spin channels is $(e^2/h)M^{\downarrow}$, i.e. the total conductance is $G^{\mathrm{AP}} = 2(e^2/h)M^{\downarrow}$. For parallel orientation of the magnetic layers the conductance is $(e^2/h)M^{\uparrow}$ if the spin direction of the carriers is the same as the magnetization, and it is $(e^2/h)M^{\downarrow}$ if the magnetization has opposite orientation to the spin orientation of the carriers. The net conductance is $G^{\mathrm{P}} = (e^2/h)(M^{\downarrow} + M^{\uparrow})$. The magnitude of the magnetoresistance effect can be characterized by $\Delta G/G^{\mathrm{P}}$, where $\Delta G = G^{\mathrm{P}} - G^{\mathrm{AP}}$. With this notation the relative change of the conductance turns out to be equal to the current spin polarization characteristic to the ferromagnetic metal applied,

$$\frac{\Delta G}{G^{\mathrm{P}}} = \frac{M^{\uparrow} - M^{\downarrow}}{M^{\uparrow} + M^{\downarrow}} = P_c. \qquad (12)$$

This simplified model corresponds to the perfectly ballistic limit, where no backscatterings are considered inside the quantum wire.

In a more realistic model the scattering inside the nanostructure should also be considered. If the structure is smaller than the phase diffusion length, l_ϕ the scattering in the two layers are added coherently, and accordingly the total resistance relies on the fine details of quantum interference phenomena.

For even larger junctions, where phase coherence between the two magnetic layers is already lost ($L > l_\phi$), but the spin information is still preserved ($L < l_s$), the two scattering regions are connected *incoherently* (Fig. 10), and accordingly their resistances are simply summed to get the total resistance.[41] In this limit the magnetoresistance of the spin valve structure is

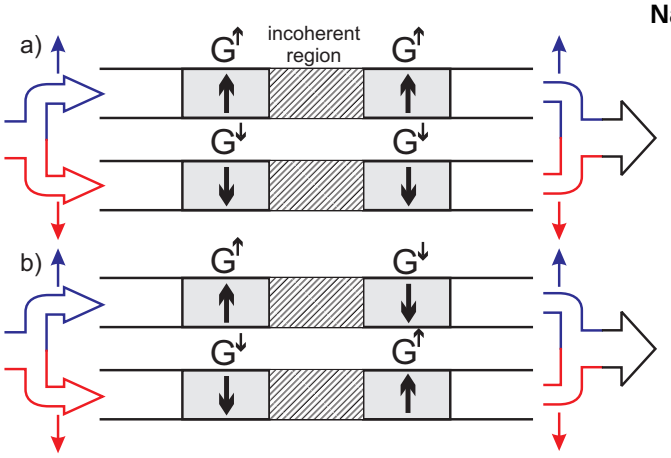

Fig. 10 *Resistive model of the GMR effect. The two magnetic layers are separated by an incoherent nonmagnetic region. The top panel demonstrates the parallel alignment of the magnetic layers (both layers have ↑ magnetization direction), whereas the bottom panel demonstrates the antiparallel alignment (the left layer has ↑ and the right layer has ↓ magnetization direction). $G^{\uparrow}$ and $G^{\downarrow}$ denote the conductance of a layer for electrons with majority and minority spin direction, respectively.*

also easily calculated. To compare with the previous ballistic model we calculate with conductances: the conductance for majority spin states is $G^{\uparrow}$, whereas for minority spins it is $G^{\downarrow}$. For antiparallel oriented magnetic layers the total conductance is $G^{AP} = 2G^{\uparrow}G^{\downarrow}/(G^{\uparrow}+G^{\downarrow})$, whereas for parallel oriented layers it is $G^{P} = G^{\uparrow}/2 + G^{\downarrow}/2$. From these equations

$$\frac{\Delta G}{G^{\mathrm{P}}} = \left(\frac{G^{\uparrow}-G^{\downarrow}}{G^{\uparrow}+G^{\downarrow}}\right)^2 = P_c^2 \qquad (13)$$

follows. Note, that this model is equivalent with the common resistor model of the GMR phenomenon.[4]

Both of the above simple models show that ΔG is positive, i.e. the parallel orientation has higher conductance than the antiparallel one. Depending on the model, the relative conductance change ranges between P_c and P_c^2 which indicates that a more complicated model based on the coherent superposition of two scattering regions would also give a result between the above two extreme limits. These considerations show that for typical values of $P_c \approx 0.2-0.6$, the relative amplitude of the GMR effect is expected to be significant regardless of the details of the model. Note, however, that this is only valid if the spin information is fully preserved in the spacer layer. As the separation of the magnetic layers becomes larger than the spin diffusion length the GMR effect exponentially decays.[8,21]

The magnetic layers of a spin valve are decoupled by paramagnetic spacer, and this allows switching between parallel and antiparallel alignments. As the relative alignment depends on the external magnetic field, the GMR effect can be used for magnetic sensing. For this purpose the orientation of one layer is pinned by growing it on top of an antiferromagnet, while the unpinned free layer can rotate even under the influence of a weak magnetic field. Spin valves are extensively applied as the read head of hard disks, which utilizes the fast and reliable reading of the magnetic information by an electric signal.

The spin valve structure can also be used to store magnetic information. This type of non-volatile memory consists of a large number of spin valves, each of them being addressed separately in a crossbar wire architecture. The orientation of the free layer defines bit "0" and bit "1", which can be changed by the stray field of the nearby crossing wires. The information written in this way is red out by the GMR effect. However, the areal density of this type of magnetoresistive random access memories (MRAM) is limited by the length scale of the slowly decreasing stray fields.

In the most advanced novel MRAMs no external field (and extra wiring) is required to write information in a spin valve memory element. In these devices the orientation of the free layer is manipulated by high density spin polarized currents, while the magnetic information is obtained by low current GMR measurements. The writing is based on the spin-flip electron scattering processes occurring in the free layer, which exert a torque on the magnetization. Even though such spin-flips are rare events (the spin diffusion length is much larger than the characteristic size of the nanodomain), at current densities of about $10^9 - 10^{10}$ A/cm^2, the induced torque becomes large enough to reverse the magnetization. The details of the spin transfer torque phenomenon are reviewed in Ref.[42]. Here we just point out the importance of the strongly non-equilibrium state of this nanoscale device: while the above current densities would lead to melting in any macroscopic metal, in this device the length scales which determine its transparency (i.e. its resistance) are well below the inelastic mean free path, and as a consequence the Joule heat is produced outside the device, in a much larger volume. In spite of the huge current densities, the nanoscale electronics defines appropriate signal levels for practical applications (below 100 μA, and around 1 V). Finally it is to be noted that the spin transfer torque magnetoresistive random access memory (STT-MRAM) is one of the most promising candidate for future spintronic applications.

5 Conclusions

Nanoscale phenomena of spin related transport were discussed both theoretically and experimentally. Based on the spin dependent band structure of a magnetic metal, we discussed the propagation of electrons in the ballistic and diffusive limits, and by applying the Landauer formalism, we supplied a *nanoscopic* background for the conventional expression of the current spin polarization. As the most direct experimen-

tal method for spin polarization measurements, the Andreev reflection spectroscopy was introduced, and experimental results on Fe and Co were shown. The analysis demonstrated the reliability of measurements carried out in the ballistic limit. The method was also extended for the determination of the spin diffusion length, one of the most important parameters of metals in spintronic applications. The operation of spin valves was described in terms of the Landauer formalism and the magnitude of the GMR effect was determined in the coherent ballistic and the incoherent diffusive limits. Finally a short overview on spin valve applications was given.

6 Acknowledgments

This work was supported by the Hungarian Research Funds OTKA under Grant Nos. 72916 and 80991. A. H. is a grantee of the Bolyai Scholarship.

Notes and references

1 S. A. Wolf, D. D. Awschalom, R. A. Buhrman, J. M. Daughton, S. von Molnr, M. L. Roukes, A. Y. Chtchelkanova and D. M. Treger, *Science*, 2001, **294**, 1488–1495.

2 D. D. Awschalom and M. E. Flatte, *Nat Phys*, 2007, **3**, 153–159.

3 I. Žutić, J. Fabian and S. Das Sarma, *Rev. Mod. Phys.*, 2004, **76**, 323–410.

4 J. F. Gregg, I. Petej, E. Jouguelet and C. Dennis, *Journal of Physics D: Applied Physics*, 2002, **35**, R121.

5 Y. V. Nazarov and Y. M. Blanter, *Quantum Transport*, Cambridge University Press, 2009.

6 S. Datta, *Electronic transport in mesoscopic systems*, Cambridge University Press, 1995.

7 J. Fabian and S. D. Sarma, *Papers from the 26th conference on the physics and chemistry of semiconductor interfaces*, 1999, **17**, 1708–1715.

8 T. Valet and A. Fert, *Phys. Rev. B*, 1993, **48**, 7099–7113.

9 R. Landauer, *Phil. Mag.*, 1970, **21**, 863–867.

10 N. Agrait, A. L. Yeyati and J. M. van Ruitenbeek, *Physics Reports*, 2003, **377**, 81 – 279.

11 B. J. van Wees, H. van Houten, C. W. J. Beenakker, J. G. Williamson, L. P. Kouwenhoven, D. van der Marel and C. T. Foxon, *Phys. Rev. Lett.*, 1988, **60**, 848–850.

12 T. Ihn, *Semiconductor Nanostructures*, Oxford University Press, 2010.

13 M. Büttiker, Y. Imry, R. Landauer and S. Pinhas, *Phys. Rev. B*, 1985, **31**, 6207–6215.

14 M. Häfner, J. K. Viljas, D. Frustaglia, F. Pauly, M. Dreher, P. Nielaba and J. C. Cuevas, *Phys. Rev. B*, 2008, **77**, 104409.

15 C. W. J. Beenakker, *Rev. Mod. Phys.*, 1997, **69**, 731–808.

16 G. T. Woods, R. J. Soulen, I. Mazin, B. Nadgorny, M. S. Osofsky, J. Sanders, H. Srikanth, W. F. Egelhoff and R. Datla, *Phys. Rev. B*, 2004, **70**, 054416.

17 R. Raue, H. Hopster and R. Clauberg, *Phys. Rev. Lett.*, 1983, **50**, 1623–1626.

18 S. Datta and B. Das, *Applied Physics Letters*, 1990, **56**, 665–667.

19 Y. Ohno, D. K. Young, B. Beschoten, F. Matsukura, H. Ohno and D. D. Awschalom, *Nature*, 1999, **402**, 790–792.

20 P. R. Hammar, B. R. Bennett, M. J. Yang and M. Johnson, *Phys. Rev. Lett.*, 1999, **83**, 203–206.

21 J. Bass and W. P. Pratt, *Journal of Physics: Condensed Matter*, 2007, **19**, 183201.

22 S. O. Valenzuela and M. Tinkham, *Nature*, 2006, **442**, 176–179.

23 P. M. Tedrow and R. Meservey, *Phys. Rev. Lett.*, 1971, **26**, 192–195.

24 R. J. Soulen Jr., J. M. Byers, M. S. Osofsky, B. Nadgorny, T. Ambrose, S. F. Cheng, P. R. Broussard, C. T. Tanaka, J. Nowak, J. S. Moodera, A. Barry and J. M. D. Coey, *Science*, 1998, **282**, 85–88.

25 S. K. Upadhyay, A. Palanisami, R. N. Louie and R. A. Buhrman, *Phys. Rev. Lett.*, 1998, **81**, 3247–3250.

26 F. Pérez-Willard, J. C. Cuevas, C. Sürgers, P. Pfundstein, J. Kopu, M. Eschrig and H. v. Löhneysen, *Phys. Rev. B*, 2004, **69**, 140502.

27 Y. Ji, G. J. Strijkers, F. Y. Yang, C. L. Chien, J. M. Byers, A. Anguelouch, G. Xiao and A. Gupta, *Phys. Rev. Lett.*, 2001, **86**, 5585–5588.

28 G. J. Strijkers, Y. Ji, F. Y. Yang, C. L. Chien and J. M. Byers, *Phys. Rev. B*, 2001, **63**, 104510.

29 C. H. Kant, O. Kurnosikov, A. T. Filip, P. LeClair, H. J. M. Swagten and W. J. M. de Jonge, *Phys. Rev. B*, 2002, **66**, 212403.

30 M. Stokmaier, G. Goll, D. Weissenberger, C. Sürgers and H. v. Löhneysen, *Phys. Rev. Lett.*, 2008, **101**, 147005.

31 T. Löfwander, R. Grein and M. Eschrig, *Phys. Rev. Lett.*, 2010, **105**, 207001.

32 A. Rajanikanth, S. Kasai, N. Ohshima and K. Hono, *Applied Physics Letters*, 2010, **97**, 022505.

33 J. G. Braden, J. S. Parker, P. Xiong, S. H. Chun and N. Samarth, *Phys. Rev. Lett.*, 2003, **91**, 056602.

34 A. Geresdi, A. Halbritter, M. Csontos, S. Csonka, G. Mihály, T. Wojtowicz, X. Liu, B. Jankó and J. K. Furdyna, *Phys. Rev. B*, 2008, **77**, 233304.

35 G. E. Blonder, M. Tinkham and T. M. Klapwijk, *Phys. Rev. B*, 1982, **25**, 4515–4532.

36 J. C. Cuevas, A. Martín-Rodero and A. L. Yeyati, *Phys. Rev. B*, 1996, **54**, 7366–7379.

37 P. Townsend and J. Sutton, *Phys. Rev.*, 1962, **128**, 591–595.

38 A. Geresdi, A. Halbritter, F. Tanczikó and G. Mihály, *Applied Physics Letters*, 2011, **98**, 212507.

39 M. N. Baibich, J. M. Broto, A. Fert, F. N. Van Dau, F. Petroff, P. Etienne, G. Creuzet, A. Friederich and J. Chazelas, *Phys. Rev. Lett.*, 1988, **61**, 2472–2475.

40 G. Binasch, P. Grünberg, F. Saurenbach and W. Zinn, *Phys. Rev. B*, 1989, **39**, 4828–4830.

41 Precisely the incoherent serial connection of two scattering regions results in the addition of the four probe resistances ($R^{4P} = R_1^{4P} + R_2^{4P}$),[6] where the four probe resistance is obtained by subtracting the contact resistance ($R^C = h/(M^{\uparrow} + M^{\downarrow})e^2$) from the two probe resistance ($R^{2P} = h/(M^{\uparrow}\overline{T}^{\uparrow} + M^{\downarrow}\overline{T}^{\downarrow})e^2$). However, considering strong scattering ($\overline{T}^{\uparrow}, \overline{T}^{\downarrow} \ll 1$) the the difference between R^{2P} and R^{4P} is negligible.

42 D. Ralph and M. Stiles, *Journal of Magnetism and Magnetic Materials*, 2008, **320**, 1190 – 1216.